

Shear-Induced Crystallization of Polypropylene. Growth Enhancement and Rheology in the Crystallization Range

Jean-Marc Haudin^{*,†}, *Catherine Duplay*[†], *Bernard Monasse*[†], *Jean-Louis Costa*[°]

[†]Ecole des Mines de Paris, CEMEF, B.P. 207, F-06904 Sophia-Antipolis Cedex, France

[°]Solvay Polyolefins Europe, Rue de Ransbeek 310, B-1120 Bruxelles, Belgium

Summary: Crystallization under shear of many different polypropylenes has been studied using a fiber pull-out device. It appears that growth can be considerably enhanced by flow. The best correlation is obtained with weight average molecular weight. Modeling the flow pattern gives access to the mechanical parameters at the growth front (shear rate and shear stress) as well as to the total strain applied to the polymer. The residual strain can be calculated taking into account relaxation processes.

Introduction

Flow-induced crystallization is a very popular topic in polymer physics. In this respect, shear flow is usually considered as a “weak” flow. However, it is able to accelerate considerably the kinetics of crystallization from the melt. This has been proved for a long time by the decrease of the induction time^[1–5], as well as by measurements of the overall kinetics.^[3,6,7] This acceleration has been generally attributed to the enhancement of the nucleation process due to flow. Conversely, the influence of shear on growth rate is less known and even ignored in some cases.

This influence has been clearly demonstrated by Monasse^[8] in the case of a polyethylene sheared between two parallel plates. Then, the question was: do analogous effects exist in polypropylene? In a first step, using the same parallel-plate device, Tribout et al.^[9] showed an increase in the growth rate after shear experiments, in spite of relaxation phenomena. Afterwards, with a fiber pull-out device this effect was also established for crystallization under shear, and a first study of the influence of molecular weight was made.^[10] This first approach was recently completed by a work underlining the major influence of the average molecular weight M_w on the growth rate under shear.^[11]

The purpose of this paper is to make a synthesis of our recent results concerning the crystallization of various polypropylenes with different molecular structures, under static and shear conditions. Static crystallizations have been carried out as a reference, for comparison with shear experiments. Growth rate has been chosen as the relevant parameter, since it makes it possible to distinguish molecular structures differences, which are not detected under static conditions.^[11,12] Furthermore, the results will be discussed using a continuum mechanics approach, which allows us to model the flow around the fiber and to calculate mechanical parameters such as the shear rate and the shear stress at the growth front as well as the total strain applied to the polymer.

Experimental

Materials

All the polymers were supplied by Solvay Polyolefins Europe. Their average molecular weights (M_n , M_w , M_z) and molecular weight distributions (MWD) were deduced from SEC measurements with a four-column Waters apparatus, at 135°C, in trichlorobenzene. Their melt flow index (MFI) was determined according to the ISO 1133 method (230°C/2.16 kg). The isotactic index (II), the amount of head-to-head or tail-to-tail defects (Rerr) and the ethylene content in copolymers were obtained by the ^{13}C NMR technique.

The polymers investigated consist of

- Ziegler-Natta (ZN) homopolymers (Table 1):

RE-PP (reactor grade): a reference series of seven polymers (L_0 to L_6) obtained with the same catalytic system under the same polymerization conditions. They have the same isotacticity index II, but different molecular weights decreasing from L_0 to L_6 ;

CR-PP (controlled rheology): polymers L_7 to L_{12} obtained by peroxidic degradation of L_1 , which affects both molecular weights and MWD;

MEL-PP: blends of L_0 and L_5 with four different compositions (% w/w: 20/80, 36/64, 50/50 and 80/20), in order to broaden MWD without changing tacticity;

BM-PP: with a bimodal distribution, also to observe the influence of MWD;

S-PP (slurry): polymerized in suspension using a different catalytic system and characterized by rather high molecular weights.

Rheological measurements

The rheological behavior of the RE-PP series in the 160-230°C temperature range has been determined with a plate-plate rheometer (Rheometrics RMS 800) in the oscillatory mode.^[12]

Table 2. Molecular characteristics of homopolymer fractions.

	<i>MFI</i>	<i>Mn</i>	<i>Mw</i>	<i>Mz</i>	<i>Mw/Mn</i>	<i>Mz/Mw</i>	<i>II (%)</i>
	g/10 min	g/mol	g/mol	g/mol			
XYL-L1	-	39 300	291 200	1 007 800	7.4	3.5	97
XYL-L2	-	26 500	260 700	919 900	9.8	3.5	97
XYL-L3	-	20 700	217 300	711 000	10.5	3.3	97
XYL-L4	-	26 000	189 300	649 800	7.3	3.4	96
XYL-L5	-	17 900	165 600	599 400	9.3	3.6	96
XYL-L6	-	15 800	139 500	525 100	8.8	3.8	98
C7-L1	-	61 000	309 400	915 800	5.1	3.0	98
C7-L2	-	41 000	272 400	801 100	6.6	2.9	98
C7-L3	-	44 500	243 200	757 500	5.5	3.1	98
C7-L4	-	35 800	211 000	653 500	5.9	3.1	98
C7-L5	-	31 700	188 200	586 500	5.9	3.1	99
C7-L6	-	20 600	161 300	545 200	7.8	3.4	98

Table 3. Molecular characteristics of metallocene homopolymers.

	<i>MFI</i>	<i>Mn</i>	<i>Mw</i>	<i>Mz</i>	<i>Mw/Mn</i>	<i>Mz/Mw</i>	<i>II (%)</i>	<i>Rem (%)</i>
	g/10 min	g/mol	g/mol	g/mol				
M1	23	41 700	129 200	234 900	3.1	1.8	93.5	0.4
M2	21	26 600	143 000	372 900	5.4	2.6	98.5	0.85
M3	22	32 300	140 000	296 500	4.3	2.1	98	0.6
M4	1.9	116 500	371 200	785 100	3.2	2.1	99	1
M5	1.1	90 300	368 500	829 700	4.1	2.3	97	0.75
M6	1.4	105 200	283 900	534 500	2.7	1.9	99	1
M7	4.3	84 000	230 900	461 100	2.7	2.0	99	1
M8	22	46 200	138 900	281 200	3.0	2.0	99	1.2
M9	45	50 400	127 000	240 900	2.5	1.9	99	1.2

Table 4. Molecular characteristics of ethylene-propylene random copolymers.

	<i>MFI</i>	<i>Mn</i>	<i>Mw</i>	<i>Mz</i>	<i>Mw/Mn</i>	<i>Mz/Mw</i>	<i>Ethylene(%)</i>
	g/10 min	g/mol	g/mol	g/mol			
CO1	2	43 000	308 800	866 000	7.2	2.8	0.6
CO2	3.5	34 500	266 500	847 000	7.7	3.2	1.4
CO3	3.4	30 400	240 400	806 100	7.9	2.8	2
CO4	2.1	30 500	311 700	1 005 300	10.2	3.2	1.7
CO5	2	38 100	299 200	887 600	7.9	3	2.8
CO6	2.2	28 500	286 800	863 700	10.1	3	3.7
CO7	1.8	31 300	288 300	908 800	9.2	3.2	6.9
CO8	2.2	68 700	307 500	866 500	4.5	2.8	1.6

The variations of the viscosity η as a function of the shear rate $\dot{\gamma}$ have been described either by a power law:

$$\eta = K \dot{\gamma}^{m-1} \quad (1)$$

where K is the consistency and m is the power-law exponent, or a by Carreau law:

$$\eta = \frac{\eta_0}{1 + (\lambda \dot{\gamma})^n} \quad (2)$$

where η_0 , λ and n are the viscosity at the Newtonian plateau, a mean relaxation time and a power-law exponent, respectively.

A spectrum of relaxation times has been calculated from the rheological measurements using a generalized Maxwell model.

All these rheological data have been extrapolated to the crystallization temperature according to an Arrhenius law.

Fiber pull-out experiments

The experimental set-up used to study crystallization under static and shear conditions is the fiber pull-out device, which is described in details elsewhere^[10,11] and sketched in Figure 1. A glass fiber is put between two polypropylene films, forming a composite material, which is placed into the hot stage, between two parallel glass slides. This composite material is heated up to 210°C, maintained at this temperature during 5 min, and cooled down to the crystallization temperature (generally 126°C) at a constant rate (-10°C/min). For static

crystallization experiments, considered as a reference, the glass fiber is immobile. For shear experiments, the fiber is fixed during the polymer cooling. As soon as the temperature reaches 126°C , the glass fiber is moved along its axis at a constant velocity $V_f = 350 \mu\text{m/s}$. This displacement induces a shear flow around the fiber.

The morphologies developed during the crystallization experiments are photographed at constant time intervals. Some basic results have been already established in previous work^[10,11] and carefully checked in the present one.^[12] When the fiber is immobile, α -spherulites are generated in the melt without any specific nucleation at the fiber surface. Due to shear, a columnar microstructure appears at the surface, consisting also of α monoclinic

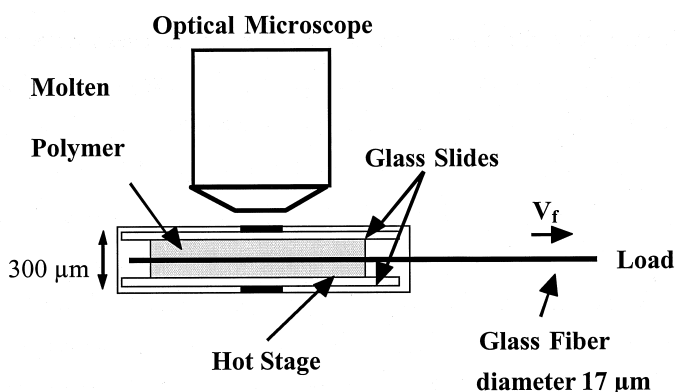


Figure 1. Fiber pull-out device.

phase. The fact that the same crystalline phase is present in both cases allows valuable comparisons between the growth rates under static and shear conditions. These growth rates correspond to the slopes of the curves giving the time variations of the radii of the bulk spherulites and of the cylindrical morphology around the fiber, respectively. They remain constant during crystallization.

Assuming a power law for the viscosity (Equation 1), Monasse^[13] has proposed a model to describe the polymer flow in the vicinity of the glass fiber. When there is no crystallization, the shear rate expression is:

$$\dot{\gamma} = \frac{1-n}{n} \frac{1}{r^{1/n}} \left[\frac{1}{r_f^{(1-1/n)} - r_e^{(1-1/n)}} \right] V_f \quad (3)$$

where r_e and r_f are the external and fiber radii, respectively; r is the location of the considered point in the polymer ($r_f \leq r \leq r_e$). The model has been extended to the case of a Carreau law^[12], but in such a case the equations have to be solved numerically. When crystallization occurs, the fiber radius has to be replaced at any time t by the radius of the solidified layer:

$$r_{sl} = r_f + Gt \quad (4)$$

G being the growth rate.

The shear stress $\tau(r)$ is given by:

$$\tau(r) = \eta \dot{\gamma}(r) \quad (5)$$

The shear stress at the growth front can be confronted to experimental values deduced from the measurements of the tensile load exerted on the fiber.

Results of growth rate measurements

Static experiments

In order to demonstrate a possible effect of molecular weight, the reference series RE-PP was first investigated, since all these polymers have the same chemical structure and differ only by their molecular weights. Taking into the precision of the measurements (about 15%), the growth rate of these polymers can be considered as independent of molecular weight. Furthermore, all the ZN homopolymers have almost the same growth rate at 126°C, our reference temperature for crystallization experiments: $G \approx 0.2 \mu\text{m/s}$ (Figure 2). These results show that molecular weight has little influence on the crystalline growth rate under static conditions. In the same way, MWD does not seem to be a significant parameter.

Nevertheless, some slight differences are observed which can be related to differences in tacticity, as confirmed by the study of the fractions (Figure 3). Regioregularity defects present in metallocene homopolymers also affect the growth rates, which are systematically lower at 126°C than the ones of their ZN homologues. Finally, the role of chain defects is obvious in the case of random copolymers. The growth rate at 126°C drastically decreases with ethylene content, and then stabilizes (Figure 4). All these results show that chain defects

(stereoregularity, regioregularity, random copolymerization) have a predominant influence on growth rate during static crystallization. In the case of metallocene homopolymers and random copolymers, this can be associated with the depression of the equilibrium melting temperature by the defects.^[12]

Shear experiments

In continuity with our previous results^[10,11], the growth rate is systematically increased by shear. This effect of flow can be quantified by the sensitivity S , which is the ratio of the growth rates under shear and static conditions: $S = G_{\text{shear}}/G_{\text{static}}$.

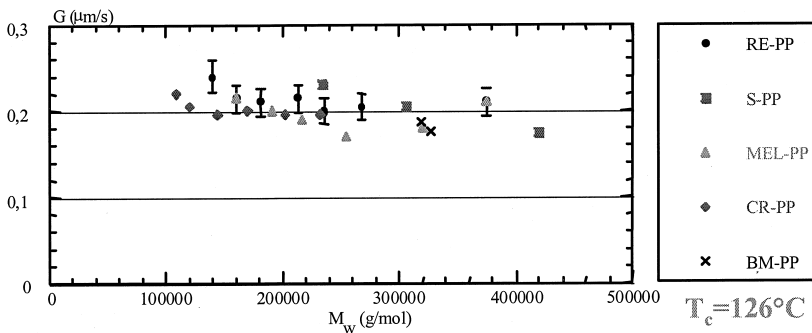


Figure 2. Influence of M_w on the growth rate of ZN homopolymers under static conditions.

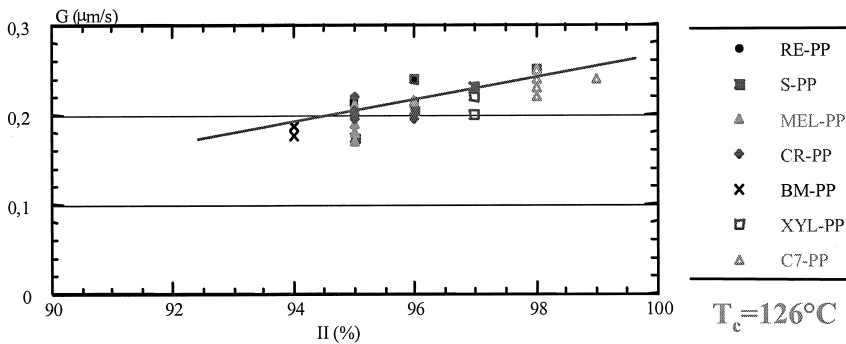


Figure 3. Influence of tacticity on the growth rate of ZN homopolymers and fractions under static conditions.

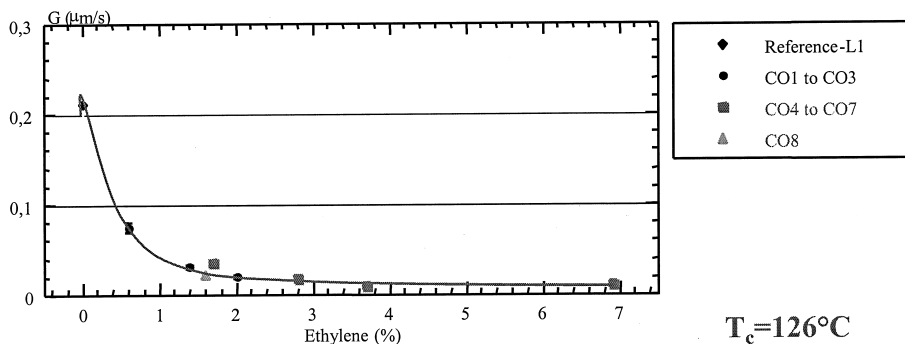


Figure 4. Influence of copolymerization on the growth rate under static conditions.

Among all the possible molecular parameters, the best correlation is found between S and the average molecular weight M_w , as shown in Figures 5 and 6 for ZN homopolymers and fractions, respectively. Furthermore, the same variation is found for metallocene homopolymers and for copolymers with a low ethylene content ($\leq 2\%$ w/w), if S is considered at the crystallization temperature where $G_{\text{static}} = 0.2 \mu\text{m/s}$ (Figures 7 and 8). Therefore, the following equation holds for all the “homopolymers”:

$$S = 0.65 \exp(7.7 \cdot 10^{-6} M_w) \quad (6)$$

with M_w in g/mol and a regression coefficient equal to 0.96.

It must be noticed that $S = 1$ for $M_w = 60\,000$ g/mol, which corresponds to a value of M_n in the 7000-17 000 g/mol range, for a polydispersity between 3.5 and 8.5. Below this critical value, which can be related to the critical mass between entanglements, the polymer should be insensitive to shear flow.

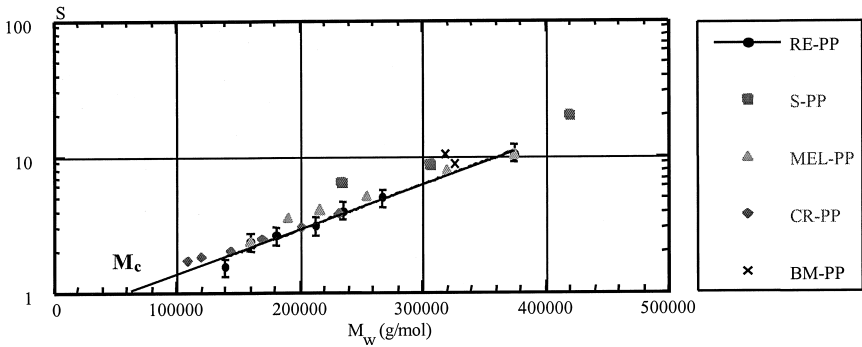


Figure 5. S vs. M_w for the ZN homopolymers.

Rheological behavior at the growth front

Shear rate and shear stress

According to the mechanical model briefly described above and using the rheological data extrapolated to the crystallization temperature, it is possible to calculate the shear rate and the shear stress at a given radius r until this point is reached by the growth point.

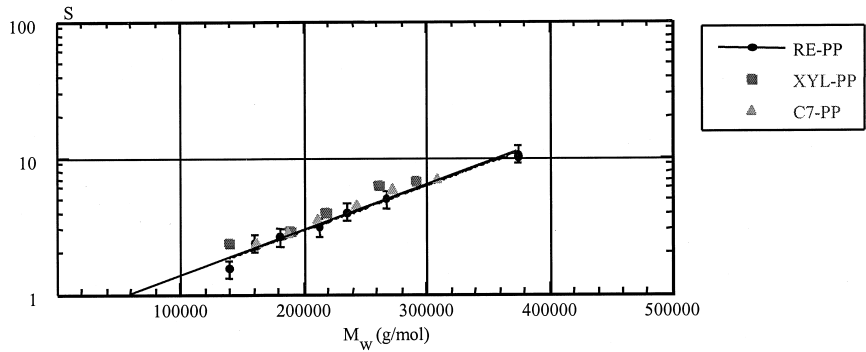


Figure 6. S vs. M_w for the fractions.

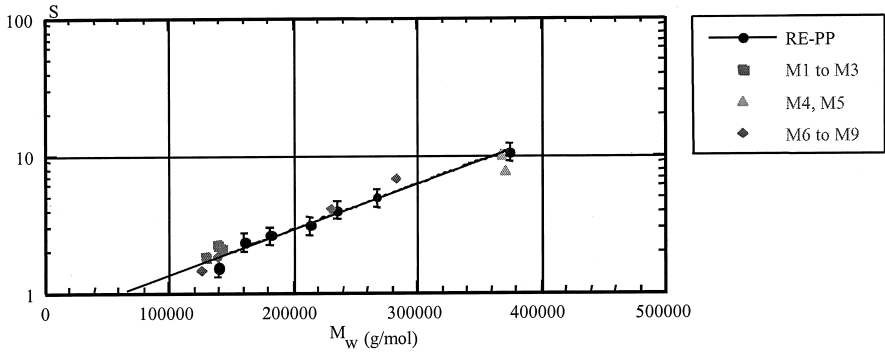


Figure 7. S vs. M_w for the metallocene homopolymers.

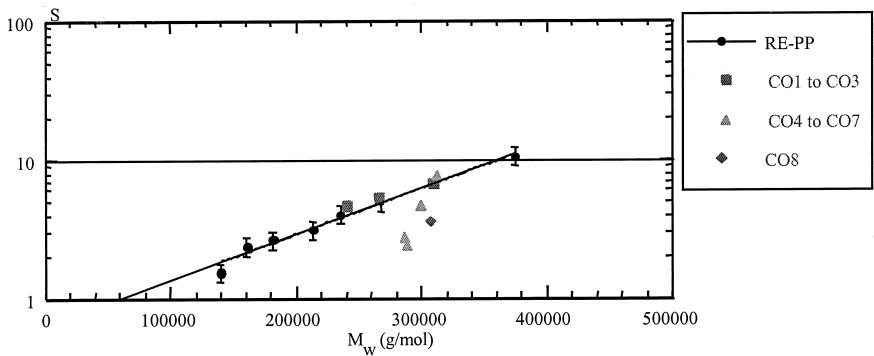


Figure 8. S vs. M_w for the random copolymers.

Whatever the radius, the shear rate increases with time, but the value at the growth front decreases (Figure 9). The shear rate at the growth front, which can be also plotted as a function of the distance to the fiber surface, is not very sensitive to the choice of the rheological law (Figure 10a).

The shear stress at the growth front also decreases with time (Figure 10b). The calculated stresses are in good agreement with the experimental values deduced from the measurement of the tensile load exerted on the fiber. This demonstrates that the flow at the front is actually a shear flow.

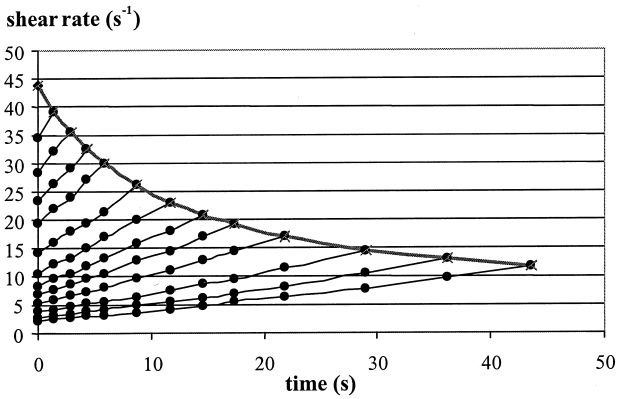
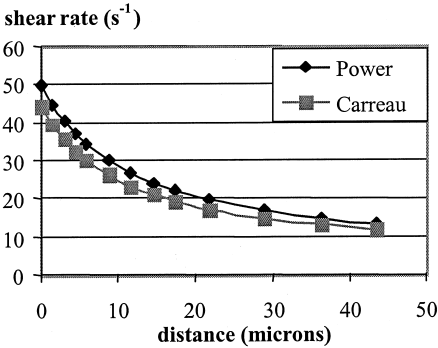
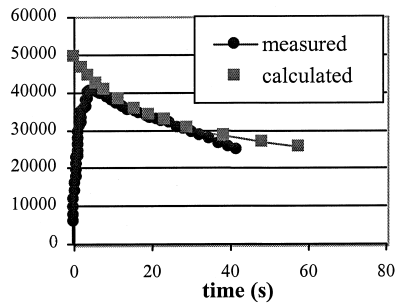


Figure 9. Variations of shear rate with time at different radii. The envelope corresponds to growth front. Polymer L_3 at 126°C .



(a)



(b)

Figure 10. Shear rate (a) and shear stress (b) at the growth front. Polymers L_3 (a) and L_5 (b).

Shear strain

Crystallization occurs under a complex shear-rate and a shear-stress history and nevertheless, the growth rate is constant. This shows that shear rate and shear stress are not relevant parameters.

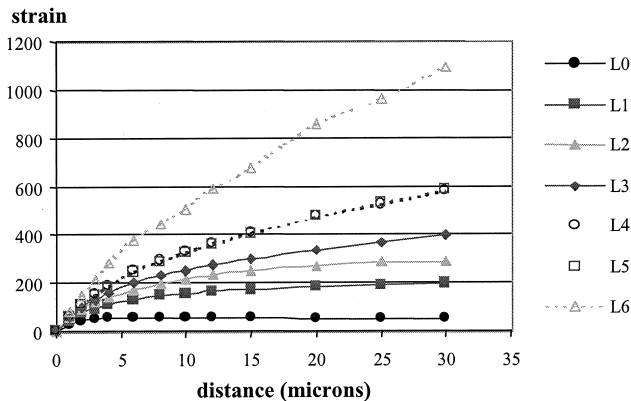


Figure 11. Evolution of shear strain for the RC-PP series at 126°C.

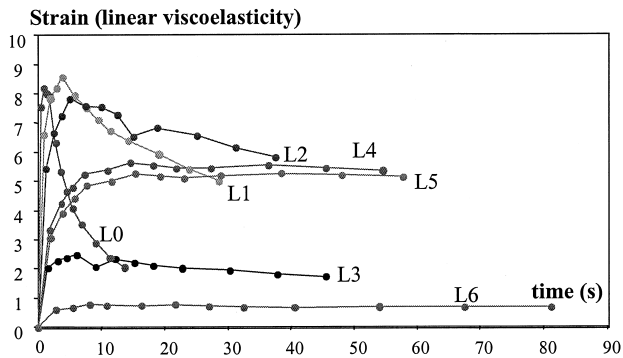


Figure 12. Shear strain at the growth front calculated using a viscoelastic model. RE-PP series at 126°C.

In a previous paper^[10], it has been pointed out that the total strain experienced by the polymer, from the beginning of shear up to solidification, stabilizes at a constant value, independent of the radius, at a certain distance from the fiber. Therefore, this cumulated strain could be a good candidate to explain the constancy of the growth rate. In the case of the RE-PP series, the strain actually stabilizes at a constant value for high molecular weight (L_0), but this is less and less true as molecular weight decreases, from L_1 to L_6 (Figure 11).

In fact, due to relaxation phenomena, the residual strain at the molecular level is lower than the one displayed in Figure 11. These relaxation phenomena are all the more important as molecular weight is low. In order to take relaxation into account, a first theoretical approach based on Lodge's viscoelastic model has been made. The relaxation modulus $G(t)$ is replaced by a memory function $m(t)$ in the equation giving the stress:

$$\tau(t) = \int_{-\infty}^t \left[\sum_{i=1}^N \frac{G_i}{\lambda_i} \exp\left(-\frac{t-t'}{\lambda_i}\right) \right] [\gamma(t) - \gamma(t')] dt' \quad (7)$$

$$\text{with } m(t-t') = \sum_{i=1}^N \frac{G_i}{\lambda_i} \exp\left(-\frac{t-t'}{\lambda_i}\right) \quad (8)$$

$$\text{and } G(t) = \int_{-\infty}^t \left[\sum_{i=1}^N \frac{G_i}{\lambda_i} \exp\left(-\frac{t-t'}{\lambda_i}\right) \right] dt' \quad (9)$$

$\gamma(t)$ is the shear strain calculated by our previous model, i.e., without taking relaxation into account. The memory function is reduced to a discrete relaxation spectrum, composed of seven elements (G_i, λ_i) (G_i : modulus; λ_i : relaxation time). It has been calculated from our experimental results and extrapolated to 126°C.

With this viscoelastic model, strain is reduced to a much lower value, about 5, even for polymer L_0 (Figure 12). A plateau is now observed for low molecular weight polymers such as L_6 . Conversely, the curves seem to be less satisfactory for L_0, L_1 and L_2 . In a general manner, the results are dispersed but it seems that the residual strain depends little on the polymer and on time.

To try to explain the dispersion of the results, different reasons may be involved:

- the use of the linear Lodge model at high strain,
- the use of a decoupled mechanical model to take into account relaxation, instead of a direct viscoelastic formulation,
- the precision of the determination of relaxation spectra, especially in the case of polymers L_0 and L_1 .

All these points would require further analysis and development.

Conclusion

It appears from the careful investigation of many different polypropylenes that:

- under static condition, growth rate is directly influenced by the molecular structure, in terms of chain regularity and defects;
- under shear, growth rate enhancement is governed by molecular weight, especially M_w .

Modeling the flow around the fiber using a continuum mechanics approach shows that this flow is actually a shear flow. The total strain applied to the polymer seems to be a pertinent parameter to describe the effects of flow on growth rate, but obviously relaxation phenomena, which are directly dependent on molecular weight, have to be taken into account.

- [1] T.W. Haas, B. Maxwell, *Polym. Eng. Sci.* **1969**, 9, 225.
- [2] D. Krueger, G.S.Y. Yeh, *J. Appl. Phys.* **1972**, 43, 4339.
- [3] A.K. Fritzsche, F.P. Price, *Polym. Eng. Sci.* **1974**, 14, 401.
- [4] R.R. Lagasse, B. Maxwell, *Polym. Eng. Sci.* **1976**, 16, 189.
- [5] V. Tan, C. Gogos, *Polym. Eng. Sci.* **1976**, 16, 512.
- [6] A.K. Fritzsche, F.P. Price, R.D. Ulrich, *Polym. Eng. Sci.* **1976**, 16, 182.
- [7] C.H. Sherwood, F.P. Price, R.S. Stein, *J. Polym. Sci. Polym. Symp.* **1978**, 63, 77.
- [8] B. Monasse, *J. Mater. Sci.* **1995**, 30, 5002.
- [9] C. Tribout, B. Monasse, J.M. Haudin, *Colloid Polym. Sci.* **1996**, 274, 197.
- [10] F. Jay, J.M. Haudin, B. Monasse, *J. Mater. Sci.* **1999**, 34, 2089.
- [11] C. Duplay, B. Monasse, J.M. Haudin, J.L. Costa, *J. Mater. Sci.* **2000**, 35, 6093.
- [12] C. Duplay, Thesis, Ecole des Mines de Paris, Sophia-Antipolis **2001**
- [13] B. Monasse, *J. Mater. Sci.* **1992**, 27, 6647.